ARCHIVES OF ELECTRICAL ENGINEERING VOL. 69(1), pp. 203–213 (2020)

DOI 10.24425/aee.2020.131768

Impact of battery cell configuration to powered wheelchair drive efficiency

KRISTAPS VITOLS, ANDREJS PODGORNOVS

Institute of Industrial Electronics and Electrical Engineering
Riga Technical University, Latvia
e-mails: {kristaps.vitols/andrejs.podgornovs}@rtu.lv

(Received: 25.04.2019, revised: 16.10.2019)

Abstract: Cells of a prototype powered wheelchair can be designed in various connections to provide different supply voltages which has impact on the efficiency of other wheelchair drive elements. The impact of cell configuration and resulting battery voltage on overall efficiency of power elements have been studied to determine the optimal configuration and voltage of the pack. A brief description of a battery energy storage system was given, and main requirements and variables were introduced to reveal the flexibility of the battery design. The efficiency versus supply voltage plots of a drive converter and battery charger were presented and discussed to find the optimal battery voltage. The motor design was analyzed from the fill factor perspective. The calculated efficiency parameters of all drive power elements were used to discuss and select an optimal battery cell configuration.

Key words: batteries, efficiency, electric vehicles, motor drives, personal mobility

1. Introduction

Power wheelchairs and other powered personal mobility aids can improve life quality of an increasing amount of human population [1, 2]. The elderly and persons with medical conditions are users of such devices. Advances in motor design, power electronics and battery technology permit improvement of such vehicles [3, 4].

Battery is one of the key points of personal mobility as it determines the driving range and price if high-cost high-performance battery technologies are used. While market analysis [5] show that lead-acid batteries are still the main energy storage solution for powered wheelchairs, the research is focusing on products which use state-of-art lithium-ion batteries [6, 7]. The use of small capacity (< 4 Ah) cells gives a degree of freedom when designing a battery pack. Such

cells can be arranged in various configurations to produce different voltages. This results in the necessity to assess the impact of battery configuration on other drive system components: a drive converter, motor and battery charger – a battery driven approach [8, 9]. Due to high costs, sizing and configuration of the battery is critical in other applications such as microgrids as well [10, 11]. Research is being carried out to improve and adjust motors to suit the needs of small vehicles and mobility devices [12, 13].

This research is a part of a lager project and the goal is to develop a modular power wheelchair which can be modified during final assembly to match the needs of user [14]. The control and user interface development is considered in [15]. Here the relevant initial data is related to the drive-power performance of the wheelchair: speed, range, acceleration, climbing capability, charging time of the battery. From previous work, it is expected for a wheelchair to have at least a 15 km driving range. The top speed will be at least 8 km/h while the drive will require no more than 320 W of power. There will be two separate drives each consisting of a motor, drive converter and battery. The motor will be able to produce at least 80 Nm torque when accelerating and climbing. The charging time will not be more than 3 h. These set-goal parameters are used as the initial data for this paper to design the battery: determine the required number of cells and their connections which sets the nominal supply voltage and current.

The paper is organized in seven sections: an introduction, which highlights the topicality and reasoning of this research; a battery energy storage system section, which is used to determine the required number of cells and to estimate internal battery losses depending on the cell connection configuration; a traction motor section, which discusses how battery voltage selection affects motor performance and construction; a drive converter section, in which calculations are made to estimate how nominal battery voltage affects converter efficiency; a battery charger section which similarly estimates efficiency of the battery charger; a discussion section uses information from the previous sections to provide a reasonable configuration of the cell connections; a conclusion section sums up all results and gives final remarks regarding the relevant design details of the battery pack.

2. Battery energy storage system

Here, the term battery energy storage system (BESS) is used to describe a set of elements which are related to energy storage. The elements of the BESS are: battery cells, cell interconnections, housing, a battery management system (BMS), charger, communication module, user application.

Li-ion cells can be commercially obtained in different cell shapes and chemistries. Energy density becomes more important when cell shape is considered. Pouch shape cells would be the best choice as the amount of packaging material is minimal and the gap between neighboring cells is small however the dimensions vary from model to model and from manufacturer to manufacturer. This shape can be used effectively for the optimal design. However, during initial research and development steps it is beneficial to use a shape that is standardized – with fixed dimensions and widely available models from different manufacturers. Due to these reasons 18650-type shape (18×65 mm cylinder) is selected for the project.

The wheelchair concept is to use two symmetric standalone drives with dedicated battery ports and battery packs. From the weight perspective, the battery pack should weigh as little as

possible so that the user is able to move the pack with a single arm. The battery will have at least 300 charge/discharge cycles [16] while capacity will be at least 300 Wh (E_{total}).

Market analysis [5] shows that several 18 650 shape models are available at capacities of 3 Ah (C_{cell}) and more. Typical nominal voltage is 3.6 V (U_{cell}). Using (1) it can be calculated that 28 cells (n_{cell}) are needed to achieve the set capacity requirement.

$$n_{cell} = \frac{E_{total}}{U_{cell} \cdot C_{cell}} \,. \tag{1}$$

If the number of cells and their model have been selected, then one can select nominal voltage of the pack. An all-parallel configuration would produce 3.6 V while series connection would produce 100.8 V. Using (2) one can calculate battery losses (P_{batt_loss}) which depends on battery current (I_{batt}) and battery internal resistance (R_{batt}).

$$P_{batt\_loss} = I_{batt}^2 \cdot R_{batt} \,. \tag{2}$$

Current depends on produced power and voltage which in turn depends on cell configuration. Equation (3) on the left shows current calculation for series connection while calculation on the right produces current for parallel connection.

$$I_{batt} = \frac{P_{batt}}{U_{cell} \cdot n_{cell}} \,, \qquad I_{batt} = \frac{P_{batt}}{U_{cell}} \,. \tag{3}$$

Each cell of the battery has its own internal resistance (R_{cell}). Equation (4) on the left produces total battery resistance for series connection while the left calculation produces resistance of parallel connection.

$$R_{batt} = R_{cell} \cdot n_{cell} \,, \qquad R_{batt} = \frac{R_{cell}}{n_{cell}} \,. \tag{4}$$

If (3) and (4) are inserted in (2) then the left side of (5) describes battery losses for series connection while the right side for parallel connection.

$$\frac{P_{batt}^2 \cdot R_{cell} \cdot n_{cell}}{U_{cell}^2 \cdot n_{cell}^2} = \frac{P_{batt}^2 \cdot R_{cell}}{U_{cell}^2 \cdot n_{cell}} \,. \tag{5}$$

Equation (5) is linear since P_{batt} and U_{cell} can be considered constant for this calculation. This means that battery losses do not depend on cell interconnections. From this perspective one could use any cell interconnection scheme. However, resulting nominal battery voltage can have effect on the efficiency and other parameters of remaining drive elements.

3. Traction motor

The design includes two motors – one for each rear wheel. Each motor is to be driven by an individual drive converter and battery pack. Motors will be designed as permanent magnet synchronous motors. The nominal voltage of the motor can be adjusted to match the one provided by the battery, thus an analysis of the motor design must be made to find the optimal voltage.

3.1. Main design boundaries

Basic motor specification values are the rated active power, rotational speed and voltage. The choice of voltage determines the required current to obtain the torque and power of the motor. The first step of the analysis is to select the values of electromagnetic loads – induction in the air gap $B\delta$, T and linear load A. The linear load is determined by the current of all armature winding turns per unit length of the stator circumference:

$$A = \frac{2m\omega I_a}{\pi D}, \tag{6}$$

where m is the number or phases, ω is the angular frequency, I_a is the armature current, D is the stator diameter.

The induction in the air gap is chosen so that the induction in the teeth does not exceed 1.4−1.8 T, and the linear load should be no more than 40 000 A/m [17].

However, for estimating electrical losses in the conductors with the known cross section it is recommended to use this value as the current density:

$$j_a = \frac{I_a}{S_{wwoi}}, \tag{7}$$

where j_a is the armature current density, S_{wwoi} is the wire cross section without insulation. It is proportional to the magnitude of the linear load $A \sim J_a$.

3.2. Armature winding slot distribution

Distributed and concentrated armature windings are considered. Conductors laid in the groove are unevenly spaced across its cross section, leaving unfilled spaces. This circumstance must be considered when determining the dimensions of the slot. If the slot is filled with a round conductor, then it can be calculated:

$$k_{fill} = \frac{n_{sl} d_{wwi}^2}{S_{sli}}, \tag{8}$$

where k_{fill} is the slot fill factor, n_{sl} is the number of slot wires, d_{wwi} is the wire diameter with insulation, S_{sli} is the insulated slot cross section.

Calculation of the fill factor gives a value of 0.785. However, a value of 0.75 is considered the most realistic for concentrated single-layer windings. The slot filling factor varies in the aisles of 0.65−0.68 for distributed windings.

When a wire is divided into elementary conductors, the fill factor drops sharply and is compared with the factor for distributed windings. However, maintaining a single conductor increases the frontal parts of the windings by increasing the allowable bending radius.

For reasons of manufacturing technology, concentrated windings are made with division into layers horizontally. The second variant with vertical winding separation [18] makes it possible to reduce the frontal parts and increase the slot filling, however, such windings are more labor-intensive in manufacturing. A slot fill factor was analyzed using conditions: constant dimensions of the motor at given power rating; constant torque. Nominal voltage is the variable parameter. For low rotational speed motors, linear load is recommended to be no more than 14.0 A/m [19]. Exceeding the linear load will reduce the efficiency of the motor and use of materials. In turn,

the slots of the motor remain unchanged and if the voltage is reduced then it is impossible to place the wire in the slot of the motor. The analysis confirmed that a motor can be designed if the nominal voltage is in the range of 18 V to 36 V. A slot fill factor limits motor design as shown in Fig. 1.

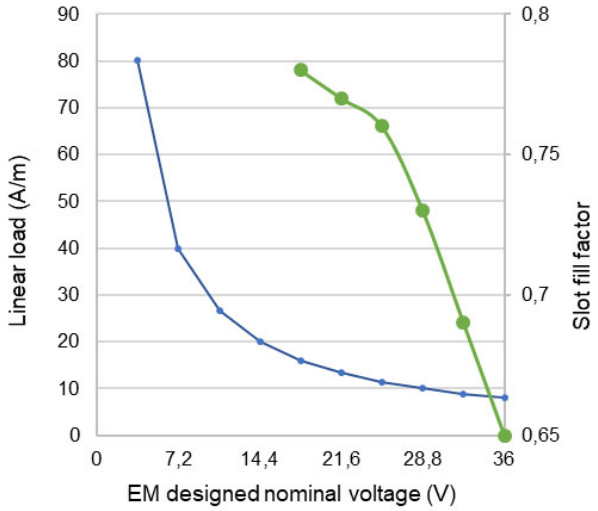

Fig. 1. Calculated linear load (grey) and armature slot fill factor (black)

4. Drive converter

A typical converter topology choice is a voltage source inverter which will be directly fed from the battery pack. The nominal voltage of the battery pack has direct impact on the electrical parameters of the inverter. If a converter will consume 320 W from the battery pack and the battery can be designed to have nominal voltage from 3.6 V to 36 V then there will be 89 A to 9 A nominal input current (I_{nom}). An analysis of commercially available switches has been performed to estimate switch losses versus nominal battery voltage. Silicon N-Chanel MOSFETs which are actively produced were used for the analysis. For each nominal voltage level (of total 10 levels) semiconductors were first filtered to have at least the required current level and minimal breakdown voltage must be at least two times higher than that of the fully charged battery pack. In most cases at least a dozen switches were selected to perform power loss calculation according to [20]. Typical buck converter signal waveforms were used to simplify calculations. Conduction losses P_{con} were calculated using (6) where R_{DSon} is the drain-source on-resistance at 10 V gate-source voltage and I_{nom} is the nominal current.

$$P_{con} = R_{DSon} \cdot I_{nom}^2 \,. \tag{9}$$

Switching losses P_{sw} are calculated using (7) where E_{on} is the energy loss per turn-on, E_{off} is the energy loss per turn-off and E_{Mrr} is the energy loss of reverse recovery of the diode. 100 kHz

switching frequency f_{sw} was used for all calculations.

$$P_{sw} = \left(E_{on} + E_{off} + E_{Mrr}\right) \cdot f_{sw} \,. \tag{10}$$

E_{on} is calculated using (8) where U_{full} is full charging voltage, I_{nom} is nominal current, t_{ri} is rise time of current and t_{fu} is fall time of voltage. E_{off} is calculated in a similar manner except that t_{ri} is replaced by t_{fi} (current fall time) and t_{fu} is replaced by t_{ru} (voltage rise time).

$$E_{on} = U_{dd} \cdot I_{nom} \cdot \frac{t_{ri} + t_{fu}}{2} + Q_{rr} \cdot U_{full} \,. \tag{11}$$

The voltage rise and fall times were calculated according to (9), where gate-drain capacitance (CGD) value was obtained from the datasheet capacitance variation graph. Datasheet current rise (t_{ri}) and fall (t_{fi}) times is far from an optimal, a better approach would be to use rise and fall times which are calculated using methods given in [21] and [22].

$$t_{fu} = \left(U_{full} - R_{DSon} \cdot I_{nom}\right) \cdot R_g \cdot \frac{C_{GD}}{U_{Dr} - U_{plateau}} \,. \tag{12}$$

Calculations were performed on several switches with lowest R_{DSon} value, several switches with lowest total gate charge value, and on several switches with lowest figure-of-merit value which is multiplication of R_{DSon} and total gate charge values. After initial examination of the results several more switches were hand-picked to find the ones with lowest losses. The obtained loss calculation results are given in Fig. 2. A total of 10 loss groups were obtained – one for each battery voltage level in 3.6 V steps. Only five lowest loss switch models are presented in the figure to provide estimation of the best-case situation. It can be concluded that above 7.2 V nominal voltage, the configuration of the battery pack has no impact on the losses of the drive's semiconductor switches.

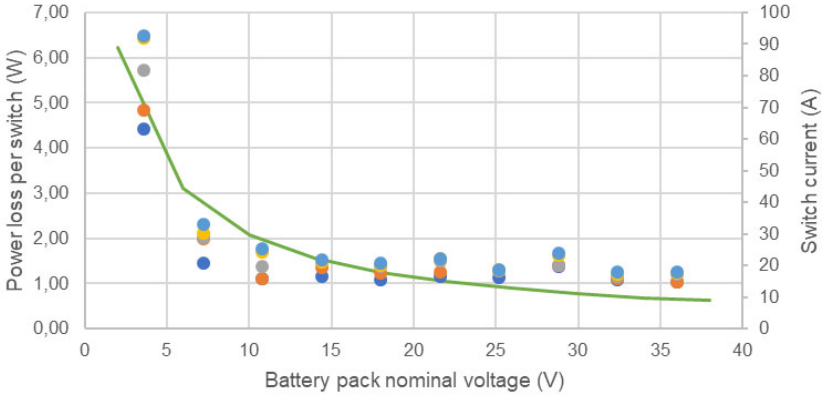

Fig. 2. Calculated power loss (dots) and current (line) per switch at different nominal battery voltages

The same MOSFET models were used to provide the 50-point cost graph shown in Fig. 3. The line presents the average for each voltage group. It can be concluded that battery configuration does not strongly affect the costs of MOSFETs for a drive converter if nominal voltage is above 7.2 V.

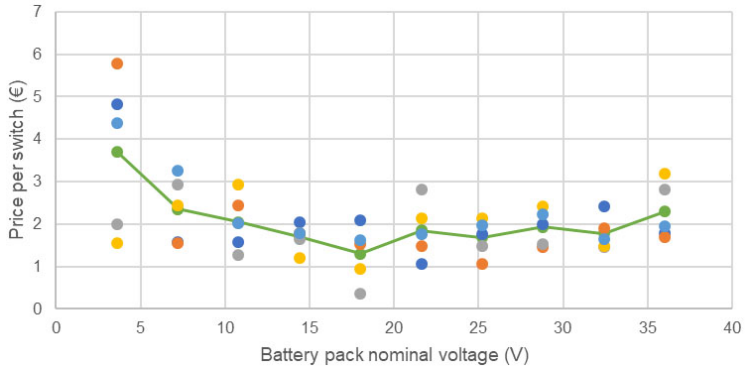

Fig. 3. Price of selected MOSFETs (dots) and average price (line) at different battery pack nominal voltages

5. Battery charger

One of the goals of the project is to design such a charging device which can simultaneously charge both battery packs. It is intended to use multi-converter isolated SEPIC (single-ended primary inductance converter) topology as shown in Fig. 4 and proposed in [23]. Generally, a charger could be designed to any battery specification, however, for this project the charger should be small in size to accomplish onboard charging while being housed in one of the armrests. Losses should be minimized to reduce charger cooling requirements hence loss calculation was performed. The AC side losses of the converter does not change if the output power remains constant – the nominal charging power is 350 W per battery. The design and component selection of the DC output side depends on the output voltage and current. As can be seen in Fig. 4, there are four identical SEPICs. Each of them has two outputs. One output is connected to the first battery while the other is connected to the second battery – converters are connected in parallel

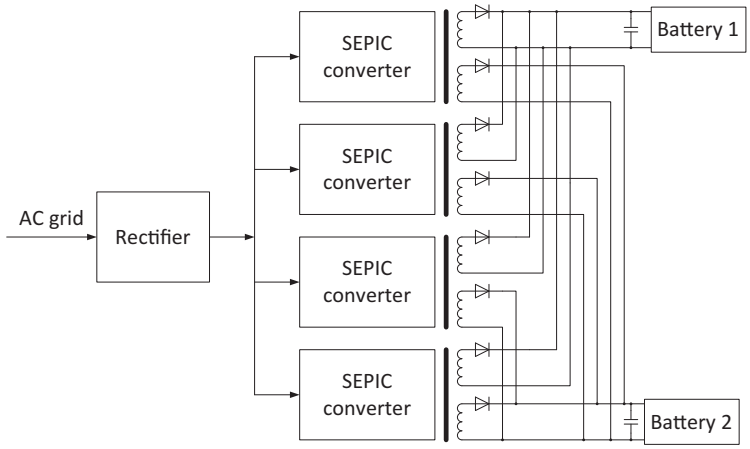

Fig. 4. Proposed layout of charger configuration

and they share a common set of output filter capacitors. Two outputs naturally operate to split output power between both batteries: the battery with lower voltage will receive more power while the other battery (with higher voltage) will charge slower. The remaining secondary side power component is a rectifier diode which will be replaced with a synchronous rectification MOSFET (metal-oxide-semiconductor field-effect transistor).

The selected MOSFETs of the previous section can be used in a synchronous rectification mode for the charger. The top 5 MOSFETs of each voltage were used to calculate losses of the charger output side. Even if just a single empty battery is connected to the charger it should be charged with 350 W – the power of each converter would be one quarter of total or 87.5 W. This power was used to calculate nominal current values of the rectifier switch at different battery nominal voltages. The obtained current levels and power losses per switch are presented in Fig. 5. It can be concluded that for battery voltage from 7.2 V to 36 V the losses are similar, and any voltage can be used as the nominal. A small exception is 28.8 V, where losses are higher due to the use of 80 V MOSFETs, which have higher R_{DSon} value than 60 V MOSFETs, which were used for 18–25.2 V nominal voltage calculations.

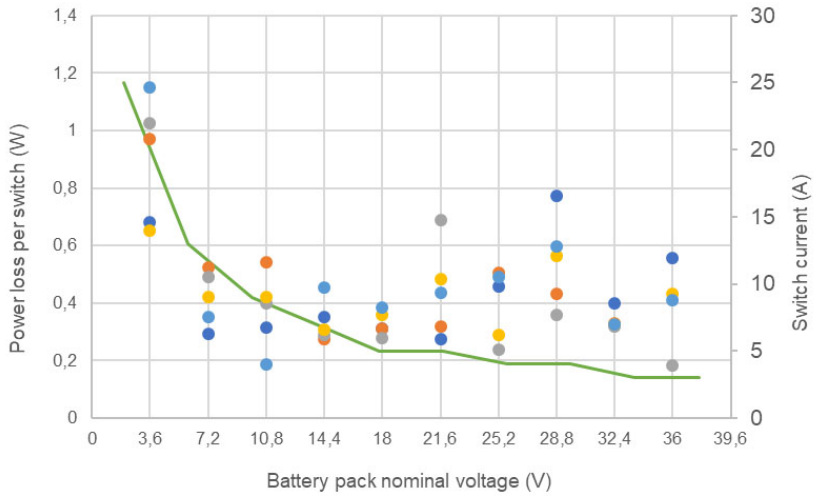

Fig. 5. Calculated power loss (dots) and current (line) per rectifier switch at different nominal battery voltages

6. Discussion

The previous sections evaluated how power losses of a motor, drive converter and battery charger change with respect to nominal voltage. The semiconductor loss calculation of a drive converter and battery charger revealed that if the battery voltage is selected to be higher than that of a single cell, the losses become almost constant (see drive losses in Table 1). The small MOSFET cost variation does not have significant impact on the selection of nominal voltage. The motor design calculations revealed that the voltage of the battery pack should be higher – at least 18 V to reach reasonable slot fill factor value.

The battery pack optimally consists of 28 cells (as established in the battery energy storage system section). The standard describing wheelchair battery packs sets the maximum nominal voltage to 36 V [16] albeit it covers only lead-acid based batteries and the limit is given for the charger. A standard covering lithium-based battery technology for wheelchairs (ISO/AWI 7176-31) is currently under development. In the case of Li-ion cells full charge voltage would reach 42 V if 10 cell series (10S) configuration is used to produce 36 V nominal voltage. This configuration would require 3 parallel cells (3P) for each level to achieve required capacity and symmetry at all levels thus the final configuration would be 10S3P and it would require 30 cells in total. Additional two cells would increase total costs and size of the battery – a disadvantage. Table 1. summarizes all configurations if a minimum of 28 cells at 3.6 V each is used. Only four configurations use optimal 28 cells. 1S28P and 2S14P configurations are to be avoided due to a high nominal current and resulting converter losses as indicated by the calculations of the drive converter section. A full charge voltage of 9S4P and 10S3P configurations exceeds 36 V – for safety, these configurations should be avoided as currently there is no standard describing a wheelchair‘s lithium-based battery. This leaves 4S7P and 7S4P configurations. 4S7P should not be used because a 14.4 V nominal voltage is not suitable for the motor design which requires the voltage to be higher than 18 V. 7S4P configuration is the best choice as the nominal voltage is high (current is low) and while losses and price of semiconductors are relatively low.

Table 1. Parameters of battery pack at different cell configurations

Nominal voltage (V)	**Full voltage (V)**	**Current (A)**	**Battery conf.**	**Required cells**	**Drive losses**	**Charger losses**	**MOSFET price**
3.6	4.2	88.9	1S28P	28	High	High	High
7.2	8.4	44.4	2S14P	28	Average	Average	Average
10.8	12.6	29.6	3S10P	30	Low	Average	Average
14.4	16.8	22.2	4S7P	28	Low	Low	Low
18	21	17.8	5S6P	30	Low	Low	Low
21.6	25.2	14.8	6S5P	30	Low	Average	Average
25.2	29.4	12.7	7S4P	28	Low	Low	Low
28.8	33.6	11.1	8S4P	32	Low	Average	Average
32.4	37.8	9.9	9S4P	36	Low	Low	Average
36	42	8.9	10S3P	30	Low	Average	Average

7. Conclusions

The efficiency of all wheelchair‘s power elements was used as the main criterion to evaluate each of the possible cell configurations of the battery. This approach yielded limited results – only the lowest voltage configurations were eliminated due to significantly higher losses and

the unrealistic slot fill factor of the motor. If the nominal voltage is higher than 7.2 V, then the absolute variation of semiconductor losses is minimal. However, this loss analysis can be used for further research when designing given converters and selecting semiconductors. From a motor design perspective, the battery voltage should be at least 18 V. The cost analysis of semiconductors provided no additional selection information. During the discussion part, the obvious conclusion was drawn that high current should be avoided as the conduction losses are quadratically proportional to the current – battery pack voltage should be as high as possible. The final cell configuration was based on the optimal cell count at maximal voltage. The 7S4P configuration has advantages: 28 cells, voltage does not exceed 36 V during charging and a 25.2 V battery pack is compatible with typically used 24 V systems which traditionally use two series connected 12 V lead-acid batteries.

Acknowledgements

The preparation of this publication is supported by the European Regional Development Fund (ERDF) within the contract No. 1.1.1.1/16/A/147 *Research and Development of Electrical, Information and Material Technologies for Low Speed Rehabilitation Vehicles for Disabled People*.

References

[1] United Nations, Department of Economic and Social Affairs, Population Division (2015), World Population Ageing 2015 (ST/ESA/SER.A/390) (2015).

[2] Whittington P., Dogan H., *SmartPowerchair: Characterization and Usability of a Pervasive System of Systems*, IEEE Trans. Human-Machine Syst., vol. 47, no. 4, pp. 500–510, August (2017).

[3] Leaman J., La H.M., *A Comprehensive Review of Smart Wheelchairs: Past, Present, and Future*, IEEE Trans. Human-Machine Syst., vol. 47, no. 4, pp. 486–499, August (2017).

[4] Podobnik J., Rejc J., Slajpah S., Munih M., Mihelj M., *All-Terrain Wheelchair: Increasing Personal Mobility with a Powered Wheel-Track Hybrid Wheelchair*, IEEE Robot. Autom. Mag., vol. 24, no. 4, pp. 26–36, December (2017).

[5] Vitols K., Podgornovs A., *Concept of cost-effective power-assist wheelchair's electrical subsystem*, in 2017 5th IEEE Workshop on Advances in Information, Electronic and Electrical Engineering (AIEEE), pp. 1–4 (2017).

[6] Yang Y.-P., Lin H.-C., Tsai F.-C., Lu C.-T., Tu K.-H., *Design and integration of dual power wheels with rim motors for a powered wheelchair*, IET Electr. Power Appl., vol. 6, no. 7, p. 419, December (2012).

[7] Lee K., Lee C.-H., Hwang S., Choi J., Bang Y., *Power-Assisted Wheelchair With Gravity and Friction Compensation*, IEEE Trans. Ind. Electron., vol. 63, no. 4, pp. 2203–2211, April (2016).

[8] Hanini N., Tabbache B., Kheloui A., Roubache T., *Sizing methodology of EV drive system based on optimal power efficiency*, in 2008 International Symposium on Power Electronics, Electrical Drives, Automation and Motion, pp. 1043–1048 (2008).

[9] Omara A.M., Sleptsov M.A., *Efficient electric traction drive configuration for battery electric vehicles*, in 2017 International Conference on Industrial Engineering, Applications and Manufacturing (ICIEAM), no. 1, pp. 1–5 (2017).

[10] Armstorfer A., Biechl H., Rosin A., *Energy Scheduling of Battery Storage Systems in Micro Grids*, Electr. Control Commun. Eng., vol. 12, no. 1, pp. 27–33, July (2017).

[11] Senfelds A., Apse-Apsitis P., Avotins A., Ribickis L., Hauf D., *Industrial DC microgrid analysis with synchronous multipoint power measurement solution*, in 2017 19th European Conference on Power Electronics and Applications (EPE'17 ECCE Europe), vol. 2017-Janua, p. P.1–P.6 (2017).

[12] Asmanis G., Ribickis L., Novikovs V., Rusko A., *Matrix frequency converter conducted and radiated emissions*, in Proceedings of the 2010 Electric Power Quality and Supply Reliability Conference, pp. 131–136 (2010).

[13] Steiks I., *The quality of the output voltage of T-type five-level converter with level shifted modulation carrier*, in 2017 IEEE 58th International Scientific Conference on Power and Electrical Engineering of Riga Technical University (RTUCON), pp. 1–4 (2017).

[14] Galkin I., Podgornovs A., Blinov A., Vitols K., Vorobyov M., Kosenko R., *Considerations Regarding the Concept of Cost-Effective Power-Assist Wheelchair Subsystems*, Electr. Control Commun. Eng., vol. 14, no. 1, pp. 71–80 (2018).

[15] Vorobyov M., Galkin I., *Concept of cost-effective power-assisted wheelchair: Human-in-the-loop subsystem*, in 2017 5th IEEE Workshop on Advances in Information, Electronic and Electrical Engineering (AIEEE), vol. 2018-Janua, no. 1, pp. 1–5 (2017).

[16] *Wheelchairs – Part 25: Batteries and chargers for powered wheelchairs*, ISO 7176-25 (2013).

[17] Kopilov I.P., *Design of Electrical Machines*, 4th ed. Moscow: Yurayt-Izdat (2011).

[18] Salminen P., Pyrhonen J., Jussila H., Niemela M., *Concentrated Wound Permanent Magnet Machines with Different Rotor Designs*, in 2007 International Conference on Power Engineering, Energy and Electrical Drives, pp. 514–517 (2007).

[19] Lifanov V.A., *Calculation of low-power electric machines with excitation from permanent magnets*, 2nd ed. Chelyabinsk: Publishing Center of SUSU (2010).

[20] Graovac D., Pürschel M., Kiep A., *MOSFET Power Losses Calculation Using the Datasheet Parameters*, Infineon, Neubiberg, Application note V1.1 (2006).

[21] *Power MOSFET Basics: Understanding Gate Charge and Using it to Assess Switching Performance*, Vishay, Malvern, Pennsylvania, Application note 73217 (2016).

[22] Lakkas G., *MOSFET power losses and how they affect power-supply efficiency*, Analog Appl. J., vol. 1, pp. 22–26 (2016).

[23] Galkin I., Blinov A., Verbytskyi I., Zinchenko D., *Modular Self-Balancing Battery Charger Concept for Cost-Effective Power-Assist Wheelchairs*, Energies, vol. 12, no. 8, p. 1526, April (2019).